Appendix

Appendix I

Isotropic and anisotropic wettability

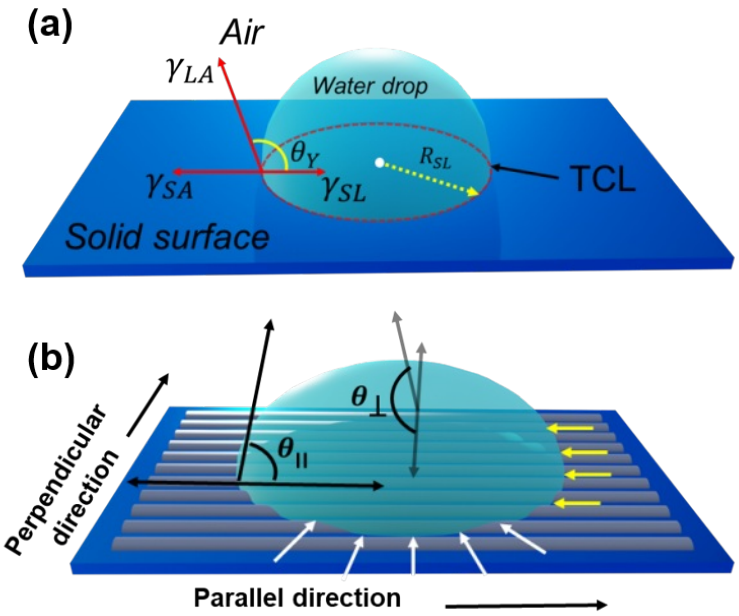

Figure A.1: Wetting states of a water droplet on solid surface: (a) Isotropic wetting. (b) Anisotropic wetting.

SEM image analysis using *Diameter-J* of *Ziziphus* leaf and biomimicked surface

We have used SEM images given in Figs. 3.5(b), 3.5(e), and 3.5(h) for segmentation in *ImageJ* analysis. The image segmentation was completed with eight different meth-

ods and was found 24 segmented images for each leaf state. The best three segmented images were chosen via visual comparing with original SEM images for further analysis. Figs. A.2(1-3) show three different segmented images and Figs. A.2(4-6) show their voids of Fig. 3.5(b) respectively for tender state leaf. Similarly, Figs. A.2(7-9), A.2(10-12) and A.2(13-15), A.2(16-18) show segmented images and void regions of Figs. 3.5(e) and 3.5(h) for mature and senescent state leaf respectively. The segmentation and porosity analysis were completed with same conditions for all three states of leaf surface. We found the porosity index ∼49-55%, 42-49%, and 45-48% for tender, mature and senescent state leaf. The estimated porosity provides good agreement with WCAs difference among three states.

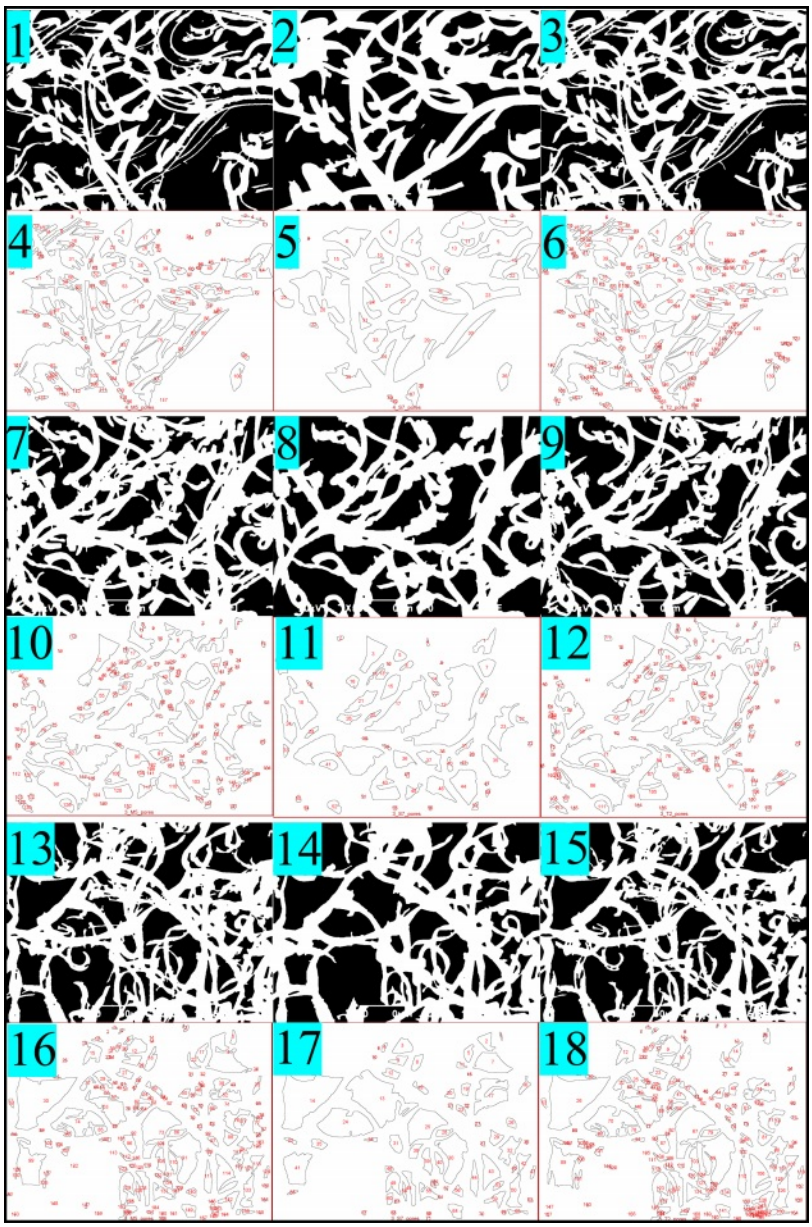

Figure A.2: *Diameter-J* analysis of *Ziziphus* leaf surface, Fig. (1-6) shows tender state leaf surface, (7-12) mature state leaf, and (13-18) senescent leaf state with different segmentation and void area; respectively.

Surface free energy calculation

According to the Kaelble-Uy model, the aforementioned theory is given by:

$$\alpha_1 x + \beta_1 y = c_1 \tag{i}$$

$$\alpha_2 x + \beta_2 y = c_2; \quad \text{where } x, y \geq 0 \tag{ii}$$

Where $x \equiv \sqrt{\gamma_s^d}$ and $y \equiv \sqrt{\gamma_s^p}$, $\alpha_1 = \sqrt{\gamma_{L_1A}^d}$ and $\alpha_2 = \sqrt{\gamma_{L_2A}^d}$, $\beta_1 = \sqrt{\gamma_{L_1A}^p}$ and $\beta_2 = \sqrt{\gamma_{L_2A}^p}$. The constants c_1 and c_2 are given by:

$$c_1 = \frac{\gamma_{L_1}^{\text{total}}(1 + \cos\theta_{L_1})}{2}, \quad c_2 = \frac{\gamma_{L_2}^{\text{total}}(1 + \cos\theta_{L_2})}{2}$$

, respectively. The total surface energy $\gamma_{L_i}^{\text{total}}$ is given by:

$$\gamma_{L_i}^{\text{total}} = \gamma_{L_iA}^d + \gamma_{L_iA}^p, \quad i = 1, 2.$$

For water:

$$\gamma_{L_1A}^d = 22.1 \text{ mJ/m}^2, \quad \gamma_{L_1A}^p = 50.7 \text{ mJ/m}^2, \quad \gamma_{L_1A}^{\text{total}} = 72.8 \text{ mJ/m}^2$$

For ethylene glycol:

$$\gamma_{L_2A}^d = 29.4 \text{ mJ/m}^2, \quad \gamma_{L_2A}^p = 18.3 \text{ mJ/m}^2, \quad \gamma_{L_2A}^{\text{total}} = 47.7 \text{ mJ/m}^2$$

Using the given values, solving Eqs. (i) and (ii), one can find out the SFE of the leaf surface (Table T.1).

Table T.1: Surface free energy (SFE) calculations based on contact angle (CA) of water and ethylene glycol for different leaf states.

Sample	**Water CA (θ°)**	**Ethylene glycol CA (θ°)**	γ_s^d **(mJ/m^2)**	γ_s^p **(mJ/m^2)**	γ_s^{total} **(mJ/m^2)**
Tender state	151.1	141.8	0.842091	0.000948	0.843039
Mature state	147.1	138.5	0.911417	0.035944	0.947361
Senescent state	143.7	133.6	1.478212	0.035879	1.514091

PVDF microfiber optimization for biommimicking of *Ziziphus* leaf surface

To optimize the fabrication of PVDF microfibers for biomimicking the matted surface structure of the *Ziziphus* leaf, two major challenges are primarily involved: (i) the preparation of bead-free fibers, and (ii) the production of nonwoven fibers with the desired diameter. To address these challenges, various electrospinning process parameters, including solution concentration, working voltage, solution flow rate, and

the distances between the needle tip and the collector, were varied across three levels. For optimization, at least ten experiments were conducted, with key parameters adjusted simultaneously to cast bead-free microfibers on the collector (Al-substrate).

(i) Solution concentration:

Electrospinning was performed using PVDF solutions with concentrations of 10 wt.%, 15 wt.%, and 20 wt.% in solvent mixtures of dimethylformamide (DMF, analytical standard, 98% pure) and acetone (analytical standard, 98% pure) at volume ratios of 1:3, 1:2, and 1:1, respectively. Beaded fibers were observed across all these combinations. Notably, partially beaded fibers were obtained at 20 wt.% PVDF with a 1:1 DMF to acetone ratio. To produce bead-free microfibers, a higher concentration of 21 wt.% PVDF was employed, which resulted in uniform, nonwoven fibers without any beads.

(ii) Working voltage:

A high voltage was applied between the conductive needle tip (∼0.55 mm) of the syringe and the collector (aluminium foil). The applied voltage was varied from 5 kV to 25 kV. At voltages below 10 kV, the resulting fibers were accompanied by beads. In contrast, at voltages above 15 kV, the fiber diameter decreased excessively, which was not desirable. An optimal voltage range of approximately 10–15 kV was identified for producing bead-free fibers with the desired diameter.

(iii) Solution flow rate:

The solution flow rate plays a critical role in the successful collection of electrospun fibers. Initially, flow rates of 1 $\mathrm{mL\,h^{-1}}$, 3 $\mathrm{mL\,h^{-1}}$, and 5 $\mathrm{mL\,h^{-1}}$ were tested, along with variations in the distance between the needle tip and the collector (∼10–15 cm). Beaded fibers were consistently observed at lower flow rates (1–3 $\mathrm{mL\,h^{-1}}$). However, at a specific tip-to-collector distance, bead-free fibers were obtained when the flow rate was increased to 6 $\mathrm{mL\,h^{-1}}$.

(iv) Collector type:

After obtaining bead-free PVDF fibers with the desired diameter using a rotating cylindrical collector (wrapped with Al- foil), the spinning speed of the collector was systematically varied in the range of approximately 200 to 800 rpm. Despite the successful fabrication of straight, uniform fibers, the resulting structures did not exhibit the intended surface morphology required for biomimicking the matted texture of the *Ziziphus* leaf. In attempt to replicate *Ziziphus* leaf matted-alike nonwoven fiber arrangements, a static plate collector (wrapped with Al- foil) was employed instead, which produced the desired fiber morphology.

By following the above steps (i) to (iv), an optimized bead-free, nonwoven microfibrous surface texture mimicking the natural structure was effectively achieved.

Dynamic water droplet states with tilting base of abaxial *Zizi-phus* leaf surface

(i) Tender state leaf surface

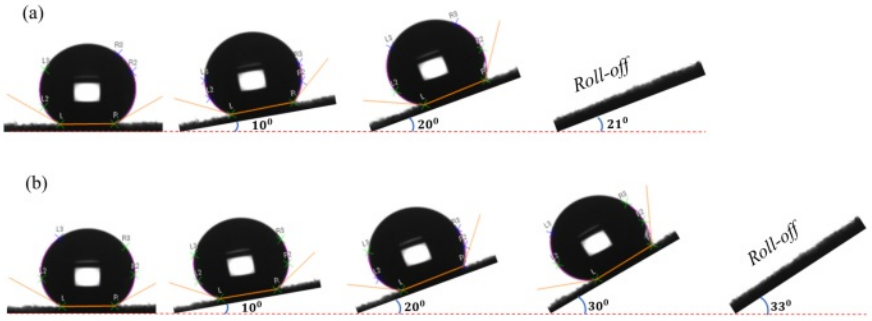

Figure A.3: Optical snaps of water droplet on abaxial surface of tender state leaf surface with tilting angles. (a) Roll off angle ∼21°. (b) Roll off angle ∼33°.

(ii) Mature state leaf surface

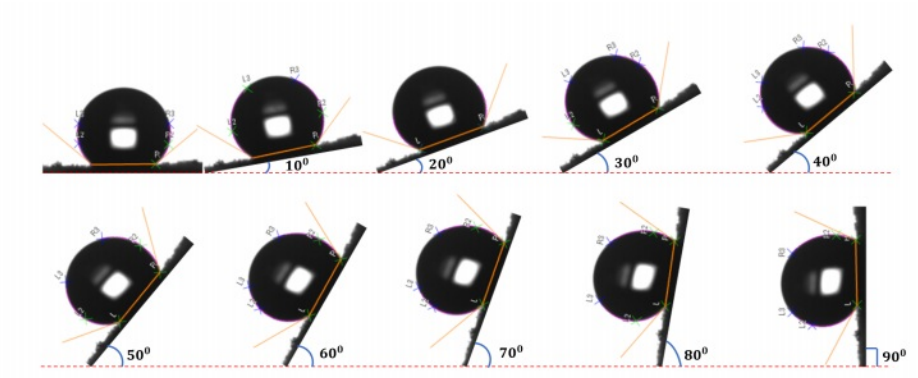

Figure A.4: Water droplet on of mature state abaxial leaf surface with tilting angle from ∼0° to ∼90°.

(iii) Senescent state leaf surface

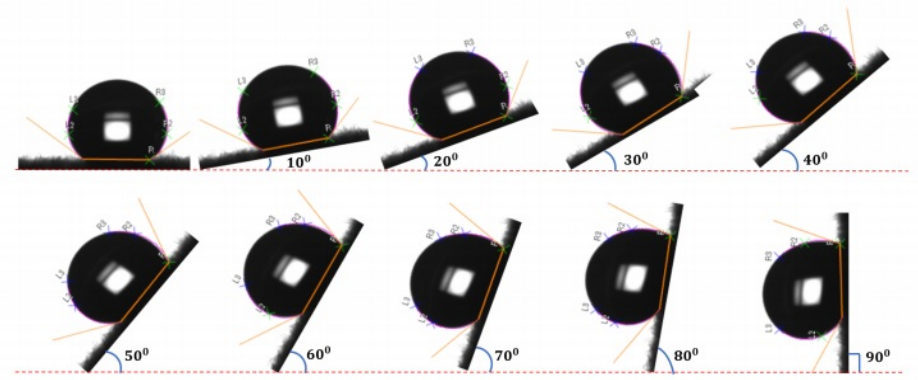

Figure A.5: Water droplet on senescent state abaxial leaf surface with tilting angle from ∼0° to ∼90°.

(iv) Fabricated PVDF microfibers surface

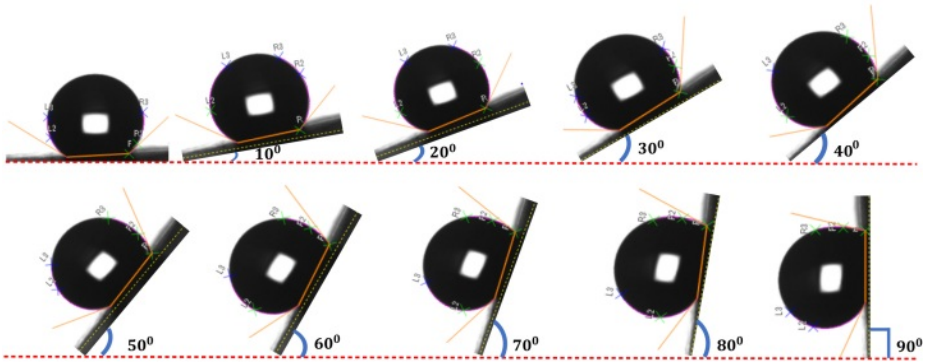

Figure A.6: Water droplet on PVDF fibrous matted surface with tilting angle varied in the range, ∼0° to ∼90°.

Appendix II

Surface roughness profile

(a) Along parallel direction

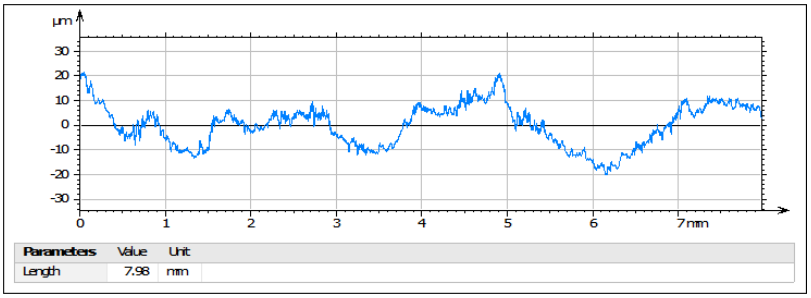

Figure A.7: Surface roughness profile of leaf specimen along parallel direction.

(b) Along perpendicular direction

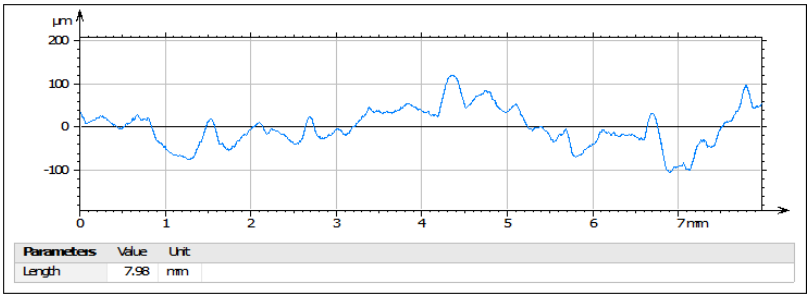

Figure A.8: Surface roughness profile of leaf specimen along perpendicular direction.

Table T.2: Roughness parameters (Along parallel direction).

Roughness Parameter	L1	L2	L3
R_q	1.95	2.29	2.48
R_a	1.57	1.83	2.05
R_z	10.1	11.2	11.9

Table T.3: Roughness parameters (Along perpendicular direction).

Roughness Parameter	L1	L2	L3
R_q	15.6	15.1	16.6
R_a	12.6	11.7	13.4
R_z	60.4	58.6	65.6

Roughness parameter estimation at different locations (L1, L2, L3) of the leaf specimen along parallel and perpendicular directions. The parameters R_q (Root-Mean-Square Deviation of the roughness), R_a (Arithmetic Mean Deviation of the roughness profile), and R_z (Maximum Height of roughness profile) values provided in tables T.2 and T.3.

Optimization steps of soft lithography for biomimeticking of sword lily leaf surface

The soft lithography techniques—based on previous studies—were introduced to fabricate biomimetic textured surfaces. During the biomimicking process, achieving specific surface textures required optimization of several parameters: the choice of material for the negative replica, the solvent used, the polymer concentration (wt.%), and careful handling of the natural leaf template. The key optimization steps are outlined below:

Preparation of negative replica

(a) Negative replica material:

In soft lithography, a negative replica is formed by molding a suitable polymer material. For artificial templates, various solvent–polymer systems can be used to create the negative replica. However, since our aim was to replicate the structure of a natural leaf, it was critical to select a polymer that dissolves in a solvent which does not chemically react with the leaf's surface, particularly its waxy outer layer. For this reason, we selected polyvinyl alcohol (PVA), a water-soluble polymer, as it preserves the integrity of the natural template.

(b) Polymer solution concentration:

PVA solutions were prepared at concentrations of 10 wt.%, 20 wt.%, and 30 wt.%. As the concentration increased, the viscosity also increased, which hindered the solution's ability to completely fill the fine features of the leaf texture. This led to incomplete or partial replication. The 10 wt.% PVA solution yielded the most promising results, producing a clear and complete negative replica. Thus, optimizing the polymer concentration is essential for successful texture replication.

(c) Leaf template, molding, and drying process:

The leaf template was placed face-up at the bottom of a glass container. The 10 wt.% PVA solution was gently poured over the leaf to ensure full coverage. To eliminate trapped air bubbles within the solution and the leaf surface texture, the setup was placed in a vacuum desiccator ($\sim$600 mm Hg) for 24 hours. After degassing, the PVA film was dried naturally at room temperature for approximately 48 hours. (Note: Accelerated drying at high temperatures was avoided to prevent damage to the natural leaf template.) Once fully dried and the water had completely evaporated, the PVA layer was carefully peeled off, resulting in a high-fidelity bio-mimicked PVA negative replica. By following steps (a–c), an optimized biomimetic surface texture can be achieved. For fabricating a positive replica, any hydrophobic polymer can be used; in this case, polystyrene (PS) was selected. The positive PS replica was prepared using the same procedure as for the negative replica. Biomimicking the sword lily leaf surface, following steps (a–c), the resulting PS replica showed a promising micro-scale

texture resembling natural specimens. However, the replica lacked the nano-scale texture present in the natural specimen, which impacted its wetting characteristics.

To address the lack of nanoscale features, future work may consider surface treatment using hydrophobic nanoparticles such as ZnO or TiO_2. These nanoparticles can be deposited onto the microtextured replica to introduce hierarchical roughness, closely resembling the micro-nanoscale architecture found in natural leaf surfaces. Such an approach is expected to enhance the wetting properties and overall biomimetic performance of the fabricated surfaces.

Lotus leaf surface microscopic image

The optical image of lotus leaf shown in Fig. A.9(a). The Figs. A.9(b-d) illustrate field emission scanning electron microscopy (FE-SEM) images of the lotus leaf surface with different magnifications. The surface micrographs reveal hierarchical micro-papillae, which are tiny protrusions covered with waxy nanostructures. These intricate features contribute to superhydrophobicity and self-cleaning of lotus leaf surface.

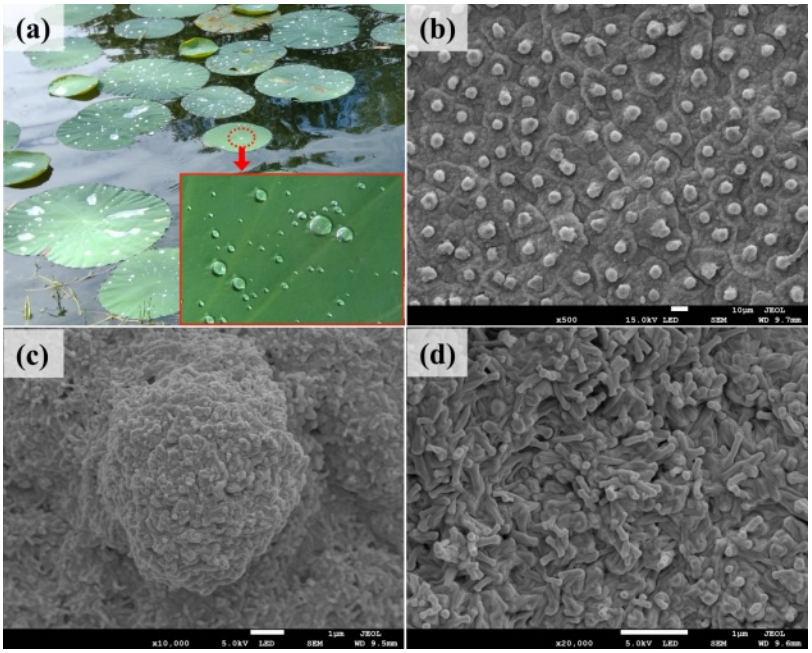

Figure A.9: (a) The optical image of natural lotus (*Nelumbo nucifera*) plant leaves. The inset show magnified top view of leaf surface containing tiny water droplets. (b) The FE-SEM images of lotus leaf surface. (c), and (d) the micro-protrusion which is covered with waxy nanostructures.

Unidirectional self-cleaning mechanism

When droplets roll in a low adhesion path that is led by a specific arrangement of micro-nano texture, this is known as directional rolling, or a directional self-cleaning process. The Fig. A.10 illustrates the self-cleaning mechanism known as the "*lotus effect* ", characterized by superhydrophobicity and low adhesion, where droplets gather

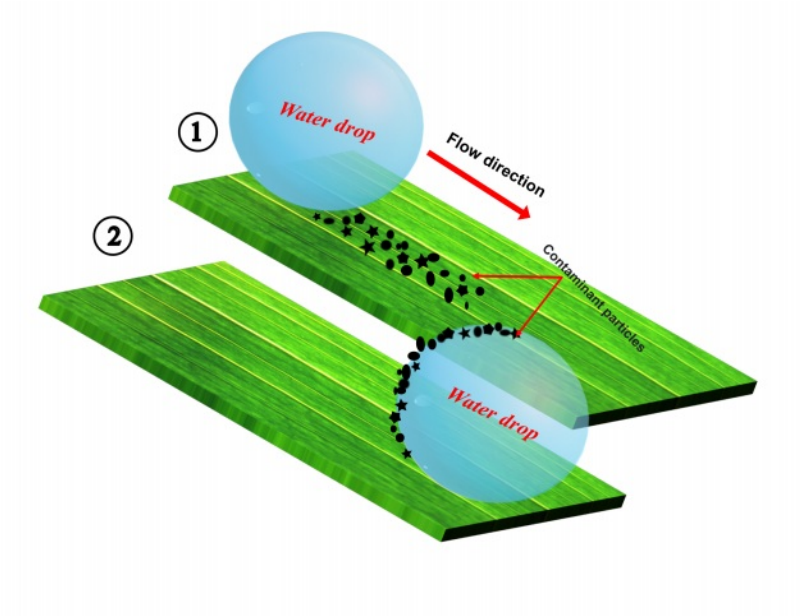

Figure A.10: The schematic depicts the low adhesion superhydrophobic unidirectional self-cleaning mechanism. The droplet would collect contaminant/particles as rolling takes places from state (1) to state (2) on a slanted stage.

and remove contaminant particles.

Micro texture Cassie- Baxter liquid-solid contact fraction

From the micrograph of the lily leaf surface, assuming a group of four micro protrusions distributed over the surface. Fig. A.11(a) shows an FE-SEM image snapshot of the lily leaf surface. The schematic in Figure Fig. A.11(b) represents the arrangements of the micro protrusions. For simplicity, we assume the wetted elliptical contact area with a and b as the minor and major axis lengths from the top view of the micro-protrusions, separated by distances c and d along the parallel and perpendicular directions, respectively. Fig. A.11(c) indicates the wetted area under the dotted shape (red color) and the rest of the vacant (air) regions. Therefore, from geometry:

$$f_{\text{micro}} = \frac{\text{Liquid-solid contact area}}{\text{Projected area}} \tag{iii}$$

or

$$f_{\text{micro}} = \frac{\pi ab}{(2b+d)(2a+c)}. \tag{iv}$$

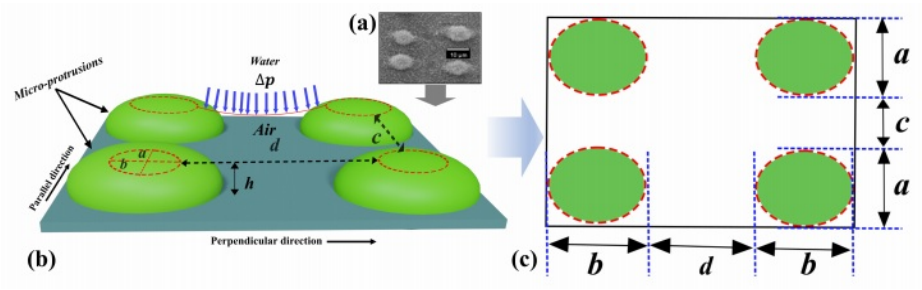

Figure A.11: The micro-protrusions geometry is assumed periodic. (a) Snapshot of FE-SEM image of natural lily leaf surface. (b) The schematic depicts the arrangements of micro-protrusions along parallel and perpendicular directions, respectively. (c) The scheme shows top view of micro-protrusions -water contact surface area under dotted region.

Appendix III

Leaf traits of selected plant species

Plant Name	Family	Characteristics	Leaf Shape & Edges
Kalanchoe fedtschenkoi	*Crassulaceae*	Succulent indoor house/garden plant; thrives in partial dry, low-intensity light areas; stores water.	Obovate shape, crenate edges; edges turn red under sunlight.
Ziziphus mauritiana	*Rhamnaceae*	Fruit plant; features thorny shrubs; survives extreme temperatures.	Oval or elliptic shape, smooth edges.
Mesua ferrea	*Calophyllaceae*	Found in tropical wet climates; tender leaves change from red/semi-transparent green to dark green.	Linear shape, smooth edges.
Litchi	*Sapindaceae*	Fruit-bearing plant; leaves are dark green on top, whitish-green below.	Lanceolate shape, smooth edges.

Table T.4: Leaf characteristics and features of selected plants

Surface morphology of plant's leaf specimens

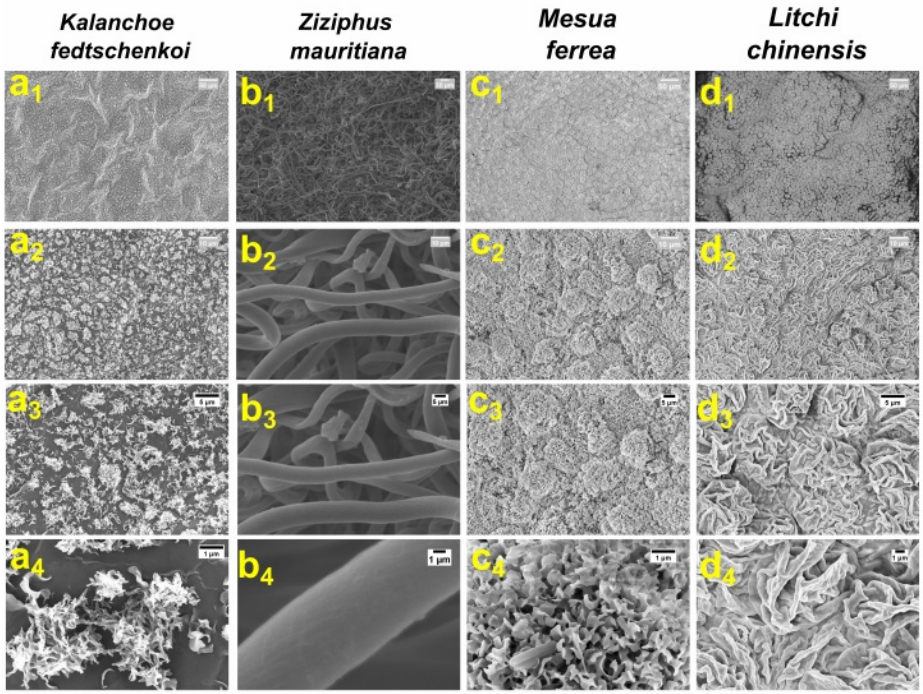

Figure A.12: SEM imaging with different magnifications of four distinct plant species (Scale: 50 μm, 10 μm, 5 μm, 1 μm). (a_1 – a_4) *Kalanchoe*, (b_1 – b_4) *Ziziphus*, (c_1 – c_4) *Mesua*, and (d_1 – d_4) *Litchi* leaf surfaces. Note the zoomed-in images from top to bottom in each column.

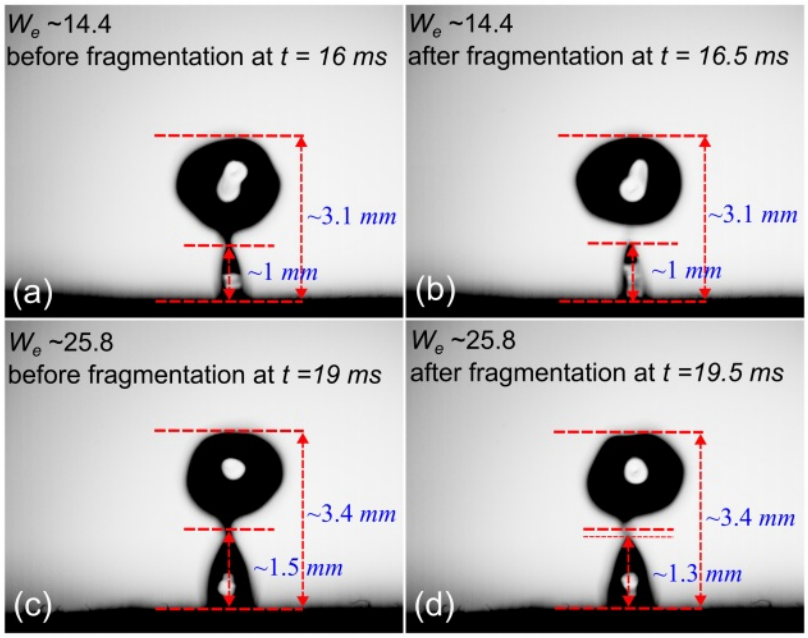

Figure A.13: Droplet fragmentation during the rebound process on hairy *Ziziphus* leaf surface. (a) and (b) show the droplet behavior before and after breakup at $We \sim 14.4$, respectively. Similarly, (c) and (d) illustrate the fragmentation process at $We \sim 25.8$.

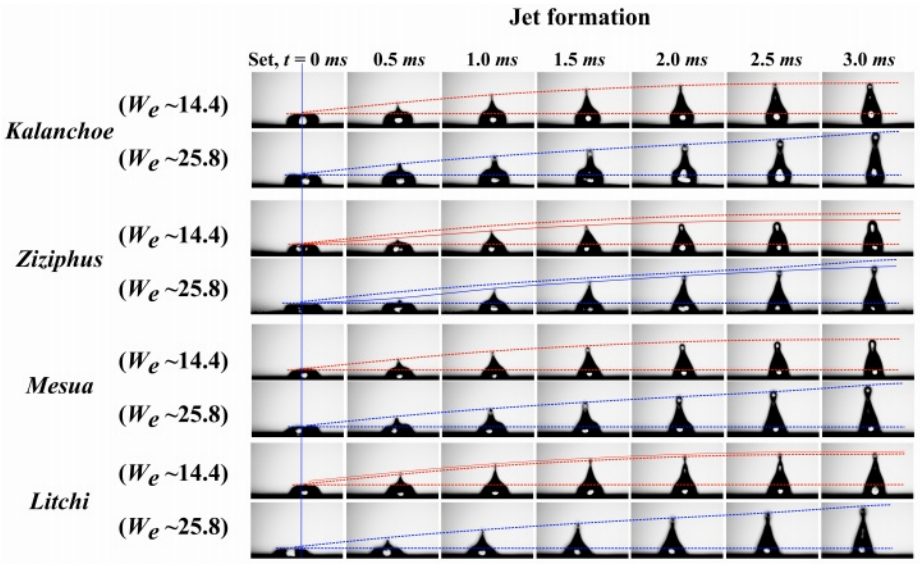

Figure A.14: High-speed imaging captures (200 *fps*, 0.5 ms) the droplet jet formation for higher Weber numbers (We ~14.4 and 25.8) on impact for all leaf surfaces. The dashed curved red (blue) color lines (top of jet) represent jet formation on the kalanchoe leaf surface and the reference line for other leaf surfaces (for We ~14.4 (~25.8)). The solid curved lines represent individual leaves' height of the jet.

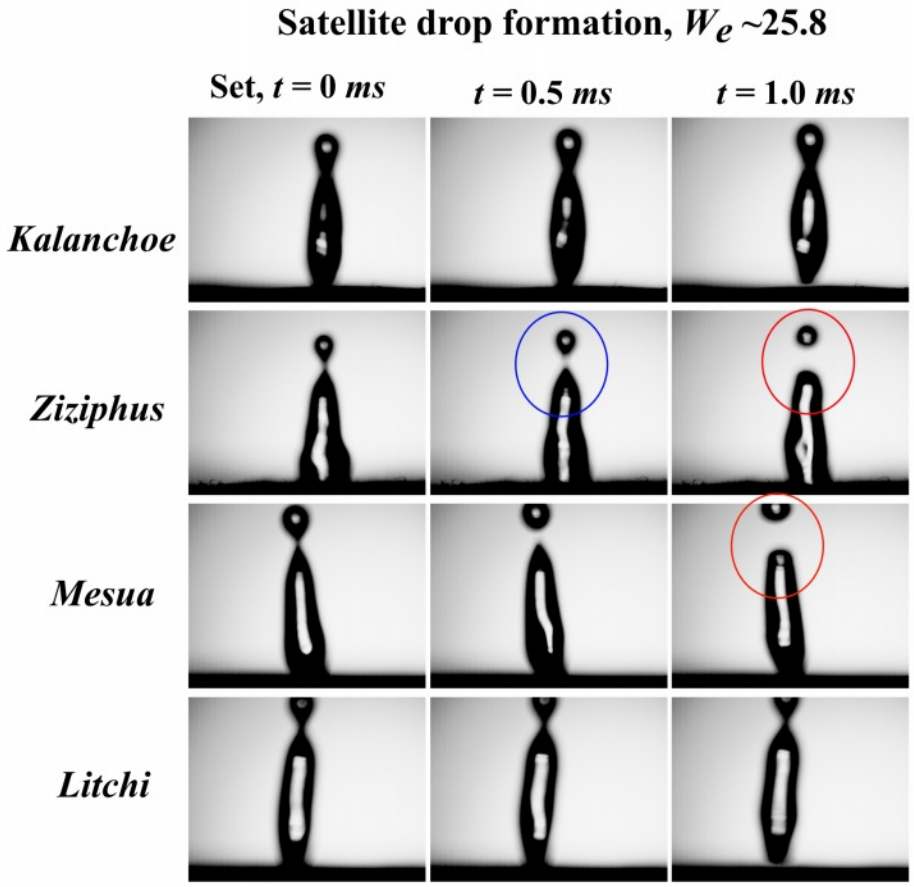

Figure A.15: High-speed imaging of satellite droplet breakup ($We \sim 25.8$). The *Kalanchoe* and *Litchi* leaf surfaces have not shown satellite droplet breakup (the occurrence of this effect may be observed for increased values of $We > 25.8$). *Ziziphus* and *Mesua* leaf surfaces possess complete satellite droplet breakup (solid red circle). The solid blue circle indicates partial detachment of the satellite droplet.

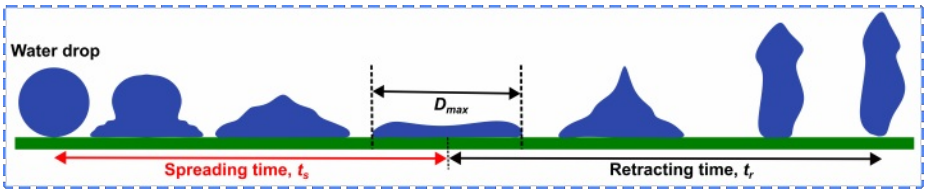

Figure A.16: The schematic illustrates droplet spreading and retraction time during bouncing experiment.

Appendix IV

Comparative analysis of surfaces

S. No.	Material	Technique	Contact Angle (°)	Notes	Reference
1	Teflon	Plasma	168		[266]
2	PDMS	Laser treatment	166		[267]
3	PS–PDMS block copolymer	Electrospinning	> 150		[268]
4	PS, PMMA	Evaporation	> 150		[269]
5	PS nanofiber	Nanoimprint	156		[270]
6	Si	Casting	158	Lotus leaf replica	[86]
7	Silica	Sol–gel	150		[271]
8	Epoxy resin + synthetic/plant waxes	Replication and self-assembly	173	Hierarchical	[272]
9	Nano-silica spheres	Dip coating	105		[273]
10	Au clusters	Electrochemical deposition	> 150		[274]
11	Carbon nanotubes	Replication and spray coating	170	Hierarchical	[275]
12	ZnO, TiO nanorods	Sol–gel	> 150	Reversible (UV irradiation)	[276]
13	PVDF	Electrospinning	145	Fibrous *Ziziphus* leaf replica	Our work
14	PS	Soft lithography	$\theta_{\parallel} \sim 130-139$, $\theta_{\perp} \sim 142-145$	Sword lily leaf replica (Hierarchical)	Our work

Table T.5: Typical materials and techniques for achieving micro-nano roughness.

Comparative analysis of biomimicked surfaces compared to natural templates

Surface characteristics	***Ziziphus* leaf**	**Biomimicked *Ziziphus* leaf surface**	**Sword lily leaf**	**Biomimicked sword lily leaf surface**
Material	Natural wax	PVDF	Natural wax	PS
Morphology	Nonwoven fibrous texture (avg. diameter ∼5.6–7.1 μm)	Nonwoven fibrous texture (avg. diameter ∼4.38 μm)	Striated three-level texture	Striated three-level texture
Texture scale	Microtexture	Microtexture	Micro-nano texture	Micro-nano texture (lacking nano texture)
Average roughness (Rq)	–	–	∼3–15 μm (parallel), ∼10–17 μm (perpendicular)	–
Porosity index	∼42–55%	∼49%	–	–
WCAs	∼143°–151°	∼145°	$\theta_{\parallel}$ ∼143°–147°, $\theta_{\perp}$ ∼156°–169°	$\theta_{\parallel}$ ∼130°–139°, $\theta_{\perp}$ ∼142°–145°
Roll-off angles	∼21°–33° (tender), no roll-off (mature/senescent)	No roll-off (up to ∼90°)	$\alpha_{\parallel}$ ∼8°–23°, $\alpha_{\perp}$ ∼16°–41°	$\alpha_{\parallel}$ ∼21°–49°, $\alpha_{\perp}$ ∼40°–55°
Contact angle hysteresis	∼30°–46°	∼49°	–	–
Critical pinning forces	–	–	∼40 μN	∼58 μN
Adhesion	High adhesion	High adhesion	–	–

Table T.6: Comparison of surface characteristics between natural and biomimicked leaf surfaces.

List of Publications

Journal Articles

1. Mahesh C. Dubey and D. Mohanta, "Coexisting superhydrophobicity and superadhesion features of *Ziziphus mauritiana* abaxial leaf surface with possibility of biomimicking using electrospun microfibers", *Physics of Fluids*, **36**(1), 017122, 2024. DOI: 10.1063/5.0176596.

2. Mahesh C. Dubey and D. Mohanta, "Exceptional anisotropic superhydrophobicity of sword-lily striated leaf surface and soft lithographic biomimicking using polystyrene replica", *Physica Scripta*, **99**(10), 105996, 2024. DOI: 10.1088/1402-4896/ad7549.

3. Mahesh C. Dubey and D. Mohanta, "Adaptive liquid lens based on electrowetting of two immiscible liquids: a study with numerical simulation and analysis", *Journal of Optics*, **52**(2), 877–884, 2023. DOI: 10.1007/s12596-022-00920-1.

Conference Article

1. Mahesh C. Dubey and D. Mohanta, "Low voltage electrowetting microlens of two immiscible liquids", *Materials Today: Proceedings*, **66**, 3412-3415, 2022. DOI: 10.1016/j.matpr.2022.07.329.

Other Article

1. Bikash K. Das, Mahesh C. Dubey, and D. Mohanta, "Blaze-angle led dark-blue iridescence and superhydrophobicity features of non-morpho *Euploea midamus* butterfly wing scale", *Physica Scripta*, **99**(5), 055039, 2024. DOI: 10.1088/1402-4896/ad3d3c.

References

[1] Petrescu, R. V., Aversa, R., Apicella, A., Kozaitis, S., Abu-Lebdeh, T., and Petrescu, F. I. NASA started a propeller set on board voyager 1 after 37 years of break. *American Journal of Engineering and Applied Sciences*, 11(1):66–77, 2018.

[2] Koh, S., Tung, C. I., Inoue, Y., and Jhanji, V. Effects of tear film dynamics on quality of vision. *British Journal of Ophthalmology*, 102(12):1615–1620, 2018.

[3] Montés-Micó, R. Role of the tear film in the optical quality of the human eye. *Journal of Cataract & Refractive Surgery*, 33(9):1631–1635, 2007.

[4] Hassall, G. The Bahá'í House of Worship: Localisation and Universal Form. In *Handbook of New Religions and Cultural Production*, pages 599–632. Brill, 2012. ISBN 90-04-22648-6.

[5] Crandell, K. E., Howe, R. O., and Falkingham, P. L. Repeated evolution of drag reduction at the air–water interface in diving kingfishers. *Journal of the Royal Society Interface*, 16(154):20190125, 2019. ISBN: 1742-5689 Publisher: The Royal Society.

[6] Lentink, D., Jongerius, S. R., and Bradshaw, N. L. The scalable design of flapping micro-air vehicles inspired by insect flight. *Flying insects and robots*, pages 185–205, 2010.

[7] Lin, P.-C., Vajpayee, S., Jagota, A., Hui, C.-Y., and Yang, S. Mechanically tunable dry adhesive from wrinkled elastomers. *Soft Matter*, 4(9):1830–1835, 2008. Publisher: Royal Society of Chemistry.

[8] Liu, K., Du, J., Wu, J., and Jiang, L. Superhydrophobic gecko feet with high adhesive forces towards water and their bio-inspired materials. *Nanoscale*, 4 (3):768–772, 2012. Publisher: Royal Society of Chemistry.

[9] Ball, P. Engineering shark skin and other solutions. *Nature*, 400(6744):507–509, 1999. ISSN 0028-0836. Publisher: Nature Publishing Group UK London.

[10] Cheng, Y. T., Rodak, D., Wong, C., and Hayden, C. Effects of micro-and nano-structures on the self-cleaning behaviour of lotus leaves. *Nanotechnology*, 17(5):1359, 2006. ISSN 0957-4484. Publisher: IOP Publishing.

[11] Bhushan, B., Jung, Y. C., and Koch, K. Self-cleaning efficiency of artificial superhydrophobic surfaces. *Langmuir*, 25(5):3240–3248, 2009. ISSN 0743-7463. Publisher: ACS Publications.

[12] Song, Y., Liu, Y., Jiang, H., Zhang, Y., Zhao, J., Han, Z., and Ren, L. Mosquito eyes inspired surfaces with robust antireflectivity and superhydrophobicity. *Surface and Coatings Technology*, 316:85–92, 2017.

[13] Gao, X., Yan, X., Yao, X., Xu, L., Zhang, K., Zhang, J., Yang, B., and Jiang, L. The dry-style antifogging properties of mosquito compound eyes and artificial analogues prepared by soft lithography. *Advanced materials*, 19(17):2213–2217, 2007.

[14] Yang, K., Liu, G., Yan, J., Wang, T., Zhang, X., and Zhao, J. A water-walking robot mimicking the jumping abilities of water striders. *Bioinspiration & biomimetics*, 11(6):066002, 2016.

[15] Hu, D. L. and Bush, J. W. The hydrodynamics of water-walking arthropods. *Journal of Fluid Mechanics*, 644:5–33, 2010.

[16] Zheng, Y., Gao, X., and Jiang, L. Directional adhesion of superhydrophobic butterfly wings. *Soft Matter*, 3(2):178–182, 2007.

[17] Lee, S. G., Lim, H. S., Lee, D. Y., Kwak, D., and Cho, K. Tunable anisotropic wettability of rice leaf-like wavy surfaces. *Advanced Functional Materials*, 23 (5):547–553, 2013. ISBN: 1616-301X Publisher: Wiley Online Library.

[18] Chen, Y.-C., Huang, Z.-S., and Yang, H. Cicada-wing-inspired self-cleaning antireflection coatings on polymer substrates. *ACS Applied Materials & Interfaces*, 7(45):25495–25505, 2015.

[19] Morikawa, J., Ryu, M., Seniutinas, G., Balčytis, A., Maximova, K., Wang, X., Zamengo, M., Ivanova, E. P., and Juodkazis, S. Nanostructured antireflective and thermoisolative cicada wings. *Langmuir*, 32(18):4698–4703, 2016.

[20] Guadarrama-Cetina, J., Mongruel, A., Medici, M. G., Baquero, E., Parker, A., Milimouk-Melnytchuk, I., González-Viñas, W., and Beysens, D. Dew condensation on desert beetle skin. *The European Physical Journal E*, 37:1–6, 2014.

[21] Nørgaard, T. and Dacke, M. Fog-basking behaviour and water collection efficiency in namib desert darkling beetles. *Frontiers in zoology*, 7:1–8, 2010.

[22] Saji, V. S. *Advances in Superhydrophobic Coatings*. Royal Society of Chemistry, 2023.

[23] Law, K.-Y. *Definitions for hydrophilicity, hydrophobicity, and superhydrophobicity: getting the basics right*, volume 5. ACS Publications, 2014. ISBN 1948-7185. Issue: 4 Pages: 686-688 Publication Title: The Journal of Physical Chemistry Letters.

[24] Li, L., Wei, J., Zhang, J., Li, B., Yang, Y., and Zhang, J. Challenges and strategies for commercialization and widespread practical applications of superhydrophobic surfaces. *Science Advances*, 9(42):eadj1554, 2023.

[25] Barthlott, W. and Neinhuis, C. Purity of the sacred lotus, or escape from contamination in biological surfaces. *Planta*, 202:1–8, 1997.

[26] Feng, L., Zhang, Y., Xi, J., Zhu, Y., Wang, N., Xia, F., and Jiang, L. Petal effect: a superhydrophobic state with high adhesive force. *Langmuir*, 24(8): 4114–4119, 2008. ISBN: 0743-7463 Publisher: ACS Publications.

[27] Cha, T.-G., Yi, J. W., Moon, M.-W., Lee, K.-R., and Kim, H.-Y. Nanoscale patterning of microtextured surfaces to control superhydrophobic robustness. *Langmuir*, 26(11):8319–8326, 2010. ISBN: 0743-7463 Publisher: ACS Publications.

[28] Liu, M., Wang, S., and Jiang, L. Bioinspired multiscale surfaces with special wettability. *MRS bulletin*, 38(5):375–382, 2013. ISBN: 0883-7694 Publisher: Cambridge University Press.

[29] Bhaumik, S. K., Chakraborty, M., Ghosh, S., Chakraborty, S., and DasGupta, S. Electric field enhanced spreading of partially wetting thin liquid films. *Langmuir*, 27(21):12951–12959, 2011.

[30] Deb, R., Sarma, B., and Dalal, A. Magnetowetting dynamics of sessile ferrofluid droplets: a review. *Soft Matter*, 18(12):2287–2324, 2022.

[31] Brutin, D. and Starov, V. Recent advances in droplet wetting and evaporation. *Chemical Society Reviews*, 47(2):558–585, 2018.

[32] Mugele, F. and Baret, J.-C. Electrowetting: from basics to applications. *Journal of physics: condensed matter*, 17(28):R705, 2005.

[33] Wang, S., Liu, K., Yao, X., and Jiang, L. Bioinspired surfaces with superwettability: new insight on theory, design, and applications. *Chemical reviews*, 115 (16):8230–8293, 2015. ISBN: 0009-2665 Publisher: ACS Publications.

[34] Wang, Y., Li, B., Bao, P., Wang, R., Min, A., and Xiong, P. A case study of leaf wettability variability and the relations with leaf traits and surface water storage for urban landscape plants. *Water*, 15(12):2152, 2023.

[35] Aryal, B. and Neuner, G. Leaf wettability decreases along an extreme altitudinal gradient. *Oecologia*, 162:1–9, 2010.

[36] Ramsukhdas, S. Srimad bhagavad gita. *Gorakhpur: Gita Press. p. ix-x*, 2014.

[37] Swarupananda, S. *Srimad Bhagavad Gita*. Advaita Ashrama (A publication branch of Ramakrishna Math, Belur Math), 2016.

[38] Bhushan, B., Jung, Y. C., and Koch, K. Micro-, nano-and hierarchical structures for superhydrophobicity, self-cleaning and low adhesion. *Philosophical Transactions of the Royal Society A: Mathematical, Physical and Engineering Sciences*, 367(1894):1631–1672, 2009. ISBN: 1364-503X Publisher: The Royal Society London.

[39] Koch, K., Bhushan, B., Jung, Y. C., and Barthlott, W. Fabrication of artificial lotus leaves and significance of hierarchical structure for superhydrophobicity and low adhesion. *Soft Matter*, 5(7):1386–1393, 2009.

[40] Bhushan, B. and Nosonovsky, M. The rose petal effect and the modes of superhydrophobicity. *Philosophical Transactions of the Royal Society A: Mathematical, Physical and Engineering Sciences*, 368(1929):4713–4728, 2010. ISBN: 1364-503X Publisher: The Royal Society Publishing.

[41] Barthlott, W., Mail, M., and Neinhuis, C. Superhydrophobic hierarchically structured surfaces in biology: evolution, structural principles and biomimetic applications. *Philosophical Transactions of the Royal Society A: Mathematical, Physical and Engineering Sciences*, 374(2073):20160191, 2016.

[42] Koch, K., Bhushan, B., and Barthlott, W. Diversity of structure, morphology and wetting of plant surfaces. *Soft matter*, 4(10):1943–1963, 2008.

[43] Klemm, D., Heublein, B., Fink, H.-P., and Bohn, A. Cellulose: fascinating biopolymer and sustainable raw material. *Angewandte chemie international edition*, 44(22):3358–3393, 2005.

[44] Heckenthaler, T., Sadhujan, S., Morgenstern, Y., Natarajan, P., Bashouti, M., and Kaufman, Y. Self-cleaning mechanism: why nanotexture and hydrophobicity matter. *Langmuir*, 35(48):15526–15534, 2019.

[45] Hassan, G., Yilbas, B. S., Al-Sharafi, A., and Al-Qahtani, H. Self-cleaning of a hydrophobic surface by a rolling water droplet. *Scientific reports*, 9(1):5744, 2019.

[46] Quan, Y.-Y., Zhang, L.-Z., Qi, R.-H., and Cai, R.-R. Self-cleaning of surfaces: the role of surface wettability and dust types. *Scientific reports*, 6(1):38239, 2016.

[47] Geyer, F., D'Acunzi, M., Sharifi-Aghili, A., Saal, A., Gao, N., Kaltbeitzel, A., Sloot, T.-F., Berger, R., Butt, H.-J., and Vollmer, D. When and how self-cleaning of superhydrophobic surfaces works. *Science advances*, 6(3):eaaw9727, 2020.

[48] Zhang, Y., Wang, T., and Lv, Y. Durable biomimetic two-tier structured superhydrophobic surface with ultralow adhesion and effective antipollution property. *Langmuir*, 39(7):2548–2557, 2023.

[49] Wooh, S., Koh, J. H., Lee, S., Yoon, H., and Char, K. Trilevel-structured superhydrophobic pillar arrays with tunable optical functions. *Advanced Functional Materials*, 24(35):5550–5556, 2014.

[50] Wang, H., Lu, H., and Zhao, W. A review of droplet bouncing behaviors on superhydrophobic surfaces: Theory, methods, and applications. *Physics of Fluids*, 35(2), 2023.

[51] Khojasteh, D., Kazerooni, M., Salarian, S., and Kamali, R. Droplet impact on superhydrophobic surfaces: A review of recent developments. *Journal of Industrial and Engineering Chemistry*, 42:1–14, 2016.

[52] Xu, Y., Tian, L., Zhu, C., and Zhao, N. Reduction in the contact time of droplet impact on superhydrophobic surface with protrusions. *Physics of Fluids*, 33(7), 2021.

[53] Malla, L. K., Patil, N. D., Bhardwaj, R., and Neild, A. Droplet bouncing and breakup during impact on a microgrooved surface. *Langmuir*, 33(38):9620–9631, 2017.

[54] Solga, A., Cerman, Z., Striffler, B. F., Spaeth, M., and Barthlott, W. The dream of staying clean: Lotus and biomimetic surfaces. *Bioinspiration & biomimetics*, 2(4):S126, 2007.

[55] Foadi, F., Vaez Allaei, S. M., Palasantzas, G., and Mohammadizadeh, M. R. Roughness-dependent wetting behavior of vapor-deposited metallic thin films. *Physical Review E*, 100(2):022804, 2019.

[56] Tudose, I. V., Comanescu, F., Pascariu, P., Bucur, S., Rusen, L., Iacomi, F., Koudoumas, E., and Suchea, M. P. Chemical and physical methods for multifunctional nanostructured interface fabrication. *Functional nanostructured interfaces for environmental and biomedical applications*, pages 15–26, 2019.

[57] Thompson, L. F. An introduction to lithography. ACS Publications, 1983.

[58] Forgacs, G. and Sun, W. *Biofabrication: micro-and nano-fabrication, printing, patterning and assemblies*. William Andrew, 2013.

[59] Wang, X., Ding, B., Yu, J., and Wang, M. Engineering biomimetic superhydrophobic surfaces of electrospun nanomaterials. *Nano today*, 6(5):510–530, 2011.

[60] Kang, H. S., Jolly, J. C., Cho, H., Kalpattu, A., Zhang, X. A., and Yang, S. Three-dimensional photoengraving of monolithic, multifaceted metasurfaces. *Advanced Materials*, 33(1):2005454, 2021.

[61] Thangadurai, T. D., Manjubaashini, N., Thomas, S., Maria, H. J., Thangadurai, T. D., Manjubaashini, N., Thomas, S., and Maria, H. J. Fabrication of nanostructures. *Nanostructured Materials*, pages 129–147, 2020.

[62] Noh, J., Lee, J.-H., Na, S., Lim, H., and Jung, D.-H. Fabrication of hierarchically micro-and nano-structured mold surfaces using laser ablation for mass production of superhydrophobic surfaces. *Japanese Journal of Applied Physics*, 49(10R):106502, 2010.

[63] Krämer, S., Fuierer, R. R., and Gorman, C. B. Scanning probe lithography using self-assembled monolayers. *Chemical Reviews*, 103(11):4367–4418, 2003.

[64] Yang, L., Akhatov, I., Mahinfalah, M., and Jang, B. Z. Nano-fabrication: A review. *Journal of the Chinese Institute of Engineers*, 30(3):441–446, 2007.

[65] Wilbur, J. L., Kumar, A., Biebuyck, H. A., Kim, E., and Whitesides, G. M. Microcontact printing of self-assembled monolayers: applications in microfabrication. *Nanotechnology*, 7(4):452, 1996.

[66] Chou, S. Y., Krauss, P. R., and Renstrom, P. J. Nanoimprint lithography. *Journal of Vacuum Science & Technology B: Microelectronics and Nanometer Structures Processing, Measurement, and Phenomena*, 14(6):4129–4133, 1996.

[67] Liu, B., He, Y., Fan, Y., and Wang, X. Fabricating super-hydrophobic lotus-leaf-like surfaces through soft-lithographic imprinting. *Macromolecular rapid communications*, 27(21):1859–1864, 2006.

[68] Ibrahim, H. M. and Klingner, A. A review on electrospun polymeric nanofibers: Production parameters and potential applications. *Polymer Testing*, 90:106647, 2020.

[69] Hou, L., Wang, N., Wu, J., Cui, Z., Jiang, L., and Zhao, Y. Bioinspired superwettability electrospun micro/nanofibers and their applications. *Advanced Functional Materials*, 28(49):1801114, 2018. ISBN: 1616-301X Publisher: Wiley Online Library.

[70] Song, J.-W. and Fan, L.-W. Understanding the effects of pressure on the contact angle of water on a silicon surface in nitrogen gas environment: Contrasts between low-and high-temperature regimes. *Journal of Colloid and Interface Science*, 607:1571–1579, 2022.

[71] Bai, Y.-H., Chiu, S.-Y., and Jiang, H.-R. Deflection of sliding droplets by dielectrophoresis force on a superhydrophobic surface. *Scientific Reports*, 14 (1):12458, 2024.

[72] Kumar, S., Martin, P., Vasilyev, G., and Zussman, E. Electrically mediated static contact angle and hysteresis of polyelectrolyte solutions. *Langmuir*, 39 (31):10872–10880, 2023.

[73] Quilliet, C. and Berge, B. Electrowetting: a recent outbreak. *Current opinion in colloid & Interface science*, 6(1):34–39, 2001.

[74] Chen, L. and Bonaccurso, E. Electrowetting—from statics to dynamics. *Advances in colloid and interface science*, 210:2–12, 2014.

[75] Zhou, W., Apkarian, R., Wang, Z. L., and Joy, D. Fundamentals of scanning electron microscopy (sem). *Scanning microscopy for nanotechnology: techniques and applications*, pages 1–40, 2007.

[76] Joy, D. C. and Joy, C. S. Low voltage scanning electron microscopy. *Micron*, 27(3-4):247–263, 1996.

[77] Nguyen, J. N. T. and Harbison, A. M. Scanning electron microscopy sample preparation and imaging. *Molecular Profiling: Methods and Protocols*, pages 71–84, 2017.

[78] Kwok, D. Y. and Neumann, A. W. Contact angle measurement and contact angle interpretation. *Advances in colloid and interface science*, 81(3):167–249, 1999.

[79] Neumann, A. and Good, R. Techniques of measuring contact angles. In *Surface and Colloid Science: Volume 11: Experimental Methods*, pages 31–91. Springer, 1979.

[80] Hebbar, R., Isloor, A., and Ismail, A. Contact angle measurements. In *Membrane characterization*, pages 219–255. Elsevier, 2017.

[81] Srinivasan, S., McKinley, G. H., and Cohen, R. E. Assessing the accuracy of contact angle measurements for sessile drops on liquid-repellent surfaces. *Langmuir*, 27(22):13582–13589, 2011.

[82] Kumar, M. and Bhardwaj, R. Wetting characteristics of colocasia esculenta (taro) leaf and a bioinspired surface thereof. *Scientific reports*, 10(1):935, 2020.

[83] Marmur, A. The lotus effect: superhydrophobicity and metastability. *Langmuir*, 20(9):3517–3519, 2004. ISBN: 0743-7463 Publisher: ACS Publications.

[84] Das, A. and Bhaumik, S. K. Fabrication of cylindrical superhydrophobic microchannels by replicating lotus leaf structures on internal walls. *Journal of Micromechanics and Microengineering*, 28(4):045011, 2018.

[85] Kostal, E., Stroj, S., Kasemann, S., Matylitsky, V., and Domke, M. Fabrication of biomimetic fog-collecting superhydrophilic–superhydrophobic surface micropatterns using femtosecond lasers. *Langmuir*, 34(9):2933–2941, 2018. ISBN: 0743-7463 Publisher: ACS Publications.

[86] Sun, M., Luo, C., Xu, L., Ji, H., Ouyang, Q., Yu, D., and Chen, Y. Artificial lotus leaf by nanocasting. *Langmuir*, 21(19):8978–8981, 2005.

[87] Bhushan, B., Jung, Y. C., Niemietz, A., and Koch, K. Lotus-like biomimetic hierarchical structures developed by the self-assembly of tubular plant waxes. *Langmuir*, 25(3):1659–1666, 2009.

[88] Gu, Z.-Z., Wei, H.-M., Zhang, R.-Q., Han, G.-Z., Pan, C., Zhang, H., Tian, X.-J., and Chen, Z.-M. Artificial silver ragwort surface. *Applied Physics Letters*, 86(20), 2005. ISBN: 0003-6951 Publisher: AIP Publishing.

[89] Ye, C., Li, M., Hu, J., Cheng, Q., Jiang, L., and Song, Y. Highly reflective superhydrophobic white coating inspired by poplar leaf hairs toward an effective "cool roof". *Energy & Environmental Science*, 4(9):3364–3367, 2011. Publisher: Royal Society of Chemistry.

[90] Zhu, D., Li, X., Zhang, G., Zhang, X., Zhang, X., Wang, T., and Yang, B. Mimicking the Rice Leaf From Ordered Binary Structures to Anisotropic Wettability. *Langmuir*, 26(17):14276–14283, 2010. ISBN: 0743-7463 Publisher: ACS Publications.

[91] Nagashima, S., Suzuki, K., Matsubara, S., and Okumura, D. Bio-inspired instability-induced hierarchical patterns having tunable anisotropic wetting properties. *Advanced Materials Interfaces*, 10(14):2300039, 2023.

[92] Wang, L., Wang, R., Wang, J., and Wong, T.-S. Compact nanoscale textures reduce contact time of bouncing droplets. *Science advances*, 6(29):eabb2307, 2020.

[93] Richard, D., Clanet, C., and Quéré, D. Contact time of a bouncing drop. *Nature*, 417(6891):811–811, 2002.

[94] Bird, J. C., Dhiman, R., Kwon, H.-M., and Varanasi, K. K. Reducing the contact time of a bouncing drop. *Nature*, 503(7476):385–388, 2013.

[95] Mats, L., Bramwell, A., Dupont, J., Liu, G., and Oleschuk, R. Electrowetting on superhydrophobic natural (colocasia) and synthetic surfaces based upon fluorinated silica nanoparticles. *Microelectronic Engineering*, 148:91–97, 2015.

[96] Feng, J.-T., Wang, F.-C., and Zhao, Y.-P. Electrowetting on a lotus leaf. *Biomicrofluidics*, 3(2), 2009.

[97] Krupenkin, T. N., Taylor, J. A., Schneider, T. M., and Yang, S. From rolling ball to complete wetting: the dynamic tuning of liquids on nanostructured surfaces. *Langmuir*, 20(10):3824–3827, 2004.

[98] Kuiper, S. and Hendriks, B. H. Variable-focus liquid lens for miniature cameras. *Applied physics letters*, 85(7):1128–1130, 2004.

[99] Berge, B. and Peseux, J. Variable focal lens controlled by an external voltage: An application of electrowetting. *The European Physical Journal E*, 3:159–163, 2000.

[100] Drelich, J. and Chibowski, E. Superhydrophilic and superwetting surfaces: definition and mechanisms of control. *Langmuir*, 26(24):18621–18623, 2010.

[101] Gao, L. and McCarthy, T. J. Contact angle hysteresis explained. *Langmuir*, 22 (14):6234–6237, 2006.

[102] Wu, L., Guo, Z., and Liu, W. Surface behaviors of droplet manipulation in microfluidics devices. *Advances in Colloid and Interface Science*, 308:102770, 2022.

[103] Shu, C., Su, Q., Li, M., Wang, Z., Yin, S., and Huang, S. Fabrication of extreme wettability surface for controllable droplet manipulation over a wide temperature range. *International Journal of Extreme Manufacturing*, 4(4): 045103, 2022.

[104] Rigoni, C., Pierno, M., Mistura, G., Talbot, D., Massart, R., Bacri, J.-C., and Abou-Hassan, A. Static magnetowetting of ferrofluid drops. *Langmuir*, 32(30): 7639–7646, 2016.

[105] Quilliet, C. and Berge, B. Electrowetting: a recent outbreak. *Current opinion in colloid & Interface science*, 6(1):34–39, 2001.

[106] Moon, H., Cho, S. K., Garrell, R. L., Kim, C.-J., et al. Low voltage electrowetting-on-dielectric. *Journal of applied physics*, 92(7):4080–4087, 2002.

[107] McHale, G., Ledesma-Aguilar, R., and Neto, C. Cassie's law reformulated: Composite surfaces from superspreading to superhydrophobic. *Langmuir*, 39 (31):11028–11035, 2023.

[108] Schönecker, C. Spreading of Complex Fluids Drops. 2022. URL https://books.rsc.org/books/edited-volume/2004/chapter/4585954.

[109] Bormashenko, E. Physics of solid–liquid interfaces: From the young equation to the superhydrophobicity. *Low Temperature Physics*, 42(8):622–635, 2016.

[110] Mugele, F. and Heikenfeld, J. Introduction to capillarity and wetting phenomena. 2019.

[111] Bush, J. 18.357 interfacial phenomena, fall 2010, 2014.

[112] PACKHAM, D. E. Surface roughness and adhesion. In *Adhesion Science and Engineering*, pages 317–349. Elsevier, 2002.

[113] Berthier, J. *Micro-drops and digital microfluidics*. William Andrew, 2012.

[114] Doi, M. *Soft matter physics*. Oxford University Press, USA, 2013.

[115] McHale, G. Cassie and wenzel: were they really so wrong? *Langmuir*, 23(15): 8200–8205, 2007.

[116] Shardt, N. and Elliott, J. A. Gibbsian thermodynamics of wenzel wetting (was wenzel wrong? revisited). *Langmuir*, 36(1):435–446, 2019.

[117] Wenzel, R. N. Surface roughness and contact angle. *The Journal of Physical Chemistry*, 53(9):1466–1467, 1949.

[118] Nosonovsky, M. On the range of applicability of the Wenzel and Cassie equations. *Langmuir*, 23(19):9919–9920, 2007. ISSN 0743-7463. Publisher: ACS Publications.

[119] Stogin, B. B., Wang, L., and Wong, T.-S. 12 designing nature-inspired liquid-repellent surfaces. *Bioinspired Structures and Design*, page 300, 2020.

[120] Milne, A. and Amirfazli, A. The Cassie equation: How it is meant to be used. *Advances in colloid and interface science*, 170(1-2):48–55, 2012. ISSN 0001-8686. Publisher: Elsevier.

[121] Kim, D., Pugno, N. M., and Ryu, S. Wetting theory for small droplets on textured solid surfaces. *Scientific reports*, 6(1):37813, 2016.

[122] Bormashenko, E. Wetting transitions on biomimetic surfaces. *Philosophical Transactions of the Royal Society A: Mathematical, Physical and Engineering Sciences*, 368(1929):4695–4711, 2010.

[123] Nosonovsky, M. and Bhushan, B. Lotus effect: roughness-induced superhydrophobicity. In *Applied Scanning Probe Methods VII: Biomimetics and Industrial Applications*, pages 1–40. Springer, 2007.

[124] Bittoun, E. and Marmur, A. The role of multiscale roughness in the lotus effect: is it essential for super-hydrophobicity? *Langmuir*, 28(39):13933–13942, 2012.

[125] Tadmor, R. Open problems in wetting phenomena: pinning retention forces. *Langmuir*, 37(21):6357–6372, 2021.

[126] Brown, R., Orr Jr, F., and Scriven, L. Static drop on an inclined plate: Analysis by the finite element method. *Journal of Colloid and Interface Science*, 73(1): 76–87, 1980.

[127] Kawasaki, K. Study of wettability of polymers by sliding of water drop. *Journal of Colloid Science*, 15(5):402–407, 1960. ISBN: 0095-8522 Publisher: Elsevier.

[128] Wu, J., Xia, J., Lei, W., and Wang, B.-p. Advanced understanding of stickiness on superhydrophobic surfaces. *Scientific reports*, 3(1):3268, 2013. ISBN: 2045-2322 Publisher: Nature Publishing Group UK London.

[129] Mohammad Karim, A. Physics of droplet impact on various substrates and its current advancements in interfacial science: A review. *Journal of Applied Physics*, 133(3), 2023.

[130] Thenarianto, C., Koh, X. Q., Lin, M., Jokinen, V., and Daniel, D. Energy loss for droplets bouncing off superhydrophobic surfaces. *Langmuir*, 39(8):3162–3167, 2023.

[131] Richard, D. and Quéré, D. Bouncing water drops. *Europhysics letters*, 50(6): 769, 2000.

[132] Bormashenko, E. and Gendelman, O. A generalized electrowetting equation: Its derivation and consequences. *Chemical Physics Letters*, 599:139–141, 2014.

[133] Kang, K. H. How electrostatic fields change contact angle in electrowetting. *Langmuir*, 18(26):10318–10322, 2002.

[134] Verheijen, H. and Prins, M. Reversible electrowetting and trapping of charge: model and experiments. *Langmuir*, 15(20):6616–6620, 1999.

[135] Dhindsa, M. S., Smith, N. R., Heikenfeld, J., Rack, P. D., Fowlkes, J. D., Doktycz, M. J., Melechko, A. V., and Simpson, M. L. Reversible electrowetting of vertically aligned superhydrophobic carbon nanofibers. *Langmuir*, 22(21): 9030–9034, 2006.

[136] Vo, Q. and Tran, T. Dynamics of droplets under electrowetting effect with voltages exceeding the contact angle saturation threshold. *Journal of Fluid Mechanics*, 925:A19, 2021.

[137] Drygiannakis, A. I., Papathanasiou, A. G., and Boudouvis, A. G. On the connection between dielectric breakdown strength, trapping of charge, and contact angle saturation in electrowetting. *Langmuir*, 25(1):147–152, 2009.

[138] Peykov, V., Quinn, A., and Ralston, J. Electrowetting: a model for contact-angle saturation. *Colloid and Polymer Science*, 278:789–793, 2000.

[139] Kedzierski, J. T., Batra, R., Berry, S., Guha, I., and Abedian, B. Validation of the trapped charge model of electrowetting contact angle saturation on lipid bilayers. *Journal of Applied Physics*, 114(2), 2013.

[140] Shapiro, B., Moon, H., Garrell, R. L., and Kim, C.-J. . Equilibrium behavior of sessile drops under surface tension, applied external fields, and material variations. *Journal of Applied Physics*, 93(9):5794–5811, 2003.

[141] Mugele, F. Fundamental challenges in electrowetting: from equilibrium shapes to contact angle saturation and drop dynamics. *Soft Matter*, 5(18):3377–3384, 2009.

[142] Vallet, M., Vallade, M., and Berge, B. Limiting phenomena for the spreading of water on polymer films by electrowetting. *The European Physical Journal B-Condensed Matter and Complex Systems*, 11:583–591, 1999.

[143] Rigoni, C., Bertoldo, S., Pierno, M., Talbot, D., Abou-Hassan, A., and Mistura, G. Division of ferrofluid drops induced by a magnetic field. *Langmuir*, 34(33): 9762–9767, 2018.

[144] Manukyan, S. and Schneider, M. Experimental investigation of wetting with magnetic fluids. *Langmuir*, 32(20):5135–5140, 2016.

[145] Song, J., Liu, H., Wan, M., Zhu, Y., and Jiang, L. Bio-inspired isotropic and anisotropic wettability on a janus free-standing polypyrrole film fabricated by interfacial electro-polymerization. *Journal of Materials Chemistry A*, 1(5): 1740–1744, 2013.

[146] Ge, P., Wang, S., Zhang, J., and Yang, B. Micro-/nanostructures meet anisotropic wetting: from preparation methods to applications. *Materials Horizons*, 7(10):2566–2595, 2020.

[147] Shirtcliffe, N., McHale, G., and Newton, M. Learning from superhydrophobic plants: The use of hydrophilic areas on superhydrophobic surfaces for droplet control. *Langmuir*, 25(24):14121–14128, 2009.

[148] Guo, Z. and Liu, W. Biomimic from the superhydrophobic plant leaves in nature: Binary structure and unitary structure. *Plant Science*, 172(6):1103–1112, 2007.

[149] Miyauchi, Y., Ding, B., and Shiratori, S. Fabrication of a silver-ragwort-leaf-like super-hydrophobic micro/nanoporous fibrous mat surface by electrospinning. *Nanotechnology*, 17(20):5151, 2006.

[150] Lin, J., Cai, Y., Wang, X., Ding, B., Yu, J., and Wang, M. Fabrication of biomimetic superhydrophobic surfaces inspired by lotus leaf and silver ragwort leaf. *Nanoscale*, 3(3):1258–1262, 2011.

[151] Chien, J. C. and Sussex, I. M. Differential regulation of trichome formation on the adaxial and abaxial leaf surfaces by gibberellins and photoperiod in arabidopsis thaliana (l.) heynh. *Plant physiology*, 111(4):1321–1328, 1996.

[152] Eller, B. M. Leaf pubescence: the significance of lower surface hairs for the spectral properties of the upper surface. *Journal of Experimental Botany*, 28 (4):1054–1059, 1977.

[153] Qian, B. and Shen, Z. Fabrication of superhydrophobic surfaces by dislocation-selective chemical etching on aluminum, copper, and zinc substrates. *Langmuir*, 21(20):9007–9009, 2005.

[154] Zhang, Y., Zhang, Z., Yang, J., Yue, Y., and Zhang, H. Fabrication of superhydrophobic surface on stainless steel by two-step chemical etching. *Chemical Physics Letters*, 797:139567, 2022.

[155] Ryu, J., Kim, K., Park, J., Hwang, B. G., Ko, Y., Kim, H., Han, J., Seo, E., Park, Y., and Lee, S. J. Nearly perfect durable superhydrophobic surfaces fabricated by a simple one-step plasma treatment. *Scientific reports*, 7(1):1981, 2017.

[156] Xi, J. and Jiang, L. Biomimic superhydrophobic surface with high adhesive forces. *Industrial & Engineering Chemistry Research*, 47(17):6354–6357, 2008.

[157] Kostal, E., Stroj, S., Kasemann, S., Matylitsky, V., and Domke, M. Fabrication of biomimetic fog-collecting superhydrophilic–superhydrophobic surface micropatterns using femtosecond lasers. *Langmuir*, 34(9):2933–2941, 2018.

[158] Pachchigar, V., Ranjan, M., and Mukherjee, S. Role of hierarchical protrusions in water repellent superhydrophobic ptfe surface produced by low energy ion beam irradiation. *Scientific Reports*, 9(1):8675, 2019.

[159] Marantan, A. and Mahadevan, L. Mechanics and statistics of the worm-like chain. *American Journal of Physics*, 86(2):86–94, 2018.

[160] Deng, T., Varanasi, K. K., Hsu, M., Bhate, N., Keimel, C., Stein, J., and Blohm, M. Nonwetting of impinging droplets on textured surfaces. *Applied Physics Letters*, 94(13), 2009.

[161] Giacomello, A., Chinappi, M., Meloni, S., and Casciola, C. M. Metastable wetting on superhydrophobic surfaces: Continuum and atomistic views<? format?> of the cassie-baxter–wenzel transition. *Physical review letters*, 109(22): 226102, 2012.

[162] Liu, B. and Lange, F. F. Pressure induced transition between superhydrophobic states: Configuration diagrams and effect of surface feature size. *Journal of colloid and interface science*, 298(2):899–909, 2006.

[163] Wang, J. and Chen, D. Criteria for entrapped gas under a drop on an ultrahydrophobic surface. *Langmuir*, 24(18):10174–10180, 2008.

[164] Cassie, A. B. D. and Baxter, S. Wettability of porous surfaces. *Transactions of the Faraday society*, 40:546–551, 1944. Publisher: Royal Society of Chemistry.

[165] Hotaling, N. A., Bharti, K., Kriel, H., and Simon Jr, C. G. Dataset for the validation and use of diameterj an open source nanofiber diameter measurement tool. *Data in brief*, 5:13–22, 2015.

[166] Fiasconaro, A. and Falo, F. Elastic traits of the extensible discrete wormlike chain model. *Physical Review E*, 107(2):024501, 2023.

[167] Domaschke, S., Zündel, M., Mazza, E., and Ehret, A. E. A 3d computational model of electrospun networks and its application to inform a reduced modelling approach. *International Journal of Solids and Structures*, 158:76–89, 2019.

[168] Brinkers, S., Dietrich, H. R., de Groote, F. H., Young, I. T., and Rieger, B. The persistence length of double stranded dna determined using dark field tethered particle motion. *The Journal of chemical physics*, 130(21), 2009.

[169] Kaelble, D. and Uy, K. A reinterpretation of organic liquid-polytetrafluoroethylene surface interactions. *The Journal of Adhesion*, 2(1): 50–60, 1970.

[170] Kaelble, D. Dispersion-polar surface tension properties of organic solids. *The Journal of Adhesion*, 2(2):66–81, 1970.

[171] Xu, W. and Choi, C.-H. From sticky to slippery droplets: Dynamics of contact line depinning<? format?> on superhydrophobic surfaces. *Physical Review Letters*, 109(2):024504, 2012.

[172] Extrand, C. and Gent, A. Retention of liquid drops by solid surfaces. *Journal of colloid and interface science*, 138(2):431–442, 1990.

[173] Varanasi, K. K., Deng, T., Hsu, M. F., and Bhate, N. Design of superhydrophobic surfaces for optimum roll-off and droplet impact resistance. In *ASME International Mechanical Engineering Congress and Exposition*, volume 48746, pages 637–645, 2008.

[174] Wier, K. A. and McCarthy, T. J. Condensation on ultrahydrophobic surfaces and its effect on droplet mobility: ultrahydrophobic surfaces are not always water repellant. *Langmuir*, 22(6):2433–2436, 2006.

[175] Zhao, X., Best, A., Liu, W., Koynov, K., Butt, H.-J., and Schönecker, C. Irregular, nanostructured superhydrophobic surfaces: Local wetting and slippage monitored by fluorescence correlation spectroscopy. *Physical Review Fluids*, 6 (5):054004, 2021.

[176] Perrin, H., Lhermerout, R., Davitt, K., Rolley, E., and Andreotti, B. Defects at the nanoscale impact contact line motion at all scales. *Physical review letters*, 116(18):184502, 2016.

[177] Chang, F.-M., Hong, S.-J., Sheng, Y.-J., and Tsao, H.-K. High contact angle hysteresis of superhydrophobic surfaces: hydrophobic defects. *Applied physics letters*, 95(6), 2009.

[178] Kubiak, K. J. and Mathia, T. G. Anisotropic wetting of hydrophobic and hydrophilic surfaces–modelling by Lattice Boltzmann method. *Procedia Engineering*, 79:45–48, 2014. ISBN: 1877-7058 Publisher: Elsevier.

[179] Liang, Y., Shu, L., Natsu, W., and He, F. Anisotropic wetting characteristics versus roughness on machined surfaces of hydrophilic and hydrophobic materials. *Applied Surface Science*, 331:41–49, 2015.

[180] Ren, Z., Yang, Z., Srinivasaraghavan Govindarajan, R., Madiyar, F., Cheng, M., Kim, D., and Jiang, Y. Two-photon polymerization of butterfly wing scale inspired surfaces with anisotropic wettability. *ACS Applied Materials & Interfaces*, 16(7):9362–9370, 2024.

[181] Wu, D., Wang, J.-N., Wu, S.-Z., Chen, Q.-D., Zhao, S., Zhang, H., Sun, H.-B., and Jiang, L. Three-level biomimetic rice-leaf surfaces with controllable anisotropic sliding. *Advanced Functional Materials*, 21(15):2927–2932, 2011. ISBN: 1616-301X Publisher: Wiley Online Library.

[182] Zou, R., Wang, J., Tang, J., Zhang, X., and Zhang, Y. Directionally guided droplets on a modular bottom-up anisotropic locally ordered nickel nanocone superhydrophobic surface. *ACS Applied Materials & Interfaces*, 13(11):13848–13860, 2021.

[183] Vrancken, R. J., Blow, M. L., Kusumaatmaja, H., Hermans, K., Prenen, A. M., Bastiaansen, C. W., Broer, D. J., and Yeomans, J. M. Anisotropic wetting and de-wetting of drops on substrates patterned with polygonal posts. *Soft Matter*, 9(3):674–683, 2013. Publisher: Royal Society of Chemistry.

[184] Chen, F., Zhang, D., Yang, Q., Wang, X., Dai, B., Li, X., Hao, X., Ding, Y., Si, J., and Hou, X. Anisotropic wetting on microstrips surface fabricated by femtosecond laser. *Langmuir*, 27(1):359–365, 2011. ISBN: 0743-7463 Publisher: ACS Publications.

[185] Chung, J. Y., Youngblood, J. P., and Stafford, C. M. Anisotropic wetting on tunable micro-wrinkled surfaces. *Soft Matter*, 3(9):1163–1169, 2007. Publisher: Royal Society of Chemistry.

[186] Gleiche, M., Chi, L. F., and Fuchs, H. Nanoscopic channel lattices with controlled anisotropic wetting. *Nature*, 403(6766):173–175, 2000. ISBN: 0028-0836 Publisher: Nature Publishing Group UK London.

[187] Hans, M., Müller, F., Grandthyll, S., Hüfner, S., and Mücklich, F. Anisotropic wetting of copper alloys induced by one-step laser micro-patterning. *Applied surface science*, 263:416–422, 2012. ISBN: 0169-4332 Publisher: Elsevier.

[188] Malvadkar, N. A., Hancock, M. J., Sekeroglu, K., Dressick, W. J., and Demirel, M. C. An engineered anisotropic nanofilm with unidirectional wetting properties. *Nature materials*, 9(12):1023–1028, 2010. ISBN: 1476-1122 Publisher: Nature Publishing Group UK London.

[189] Ma, C., Bai, S., Peng, X., and Meng, Y. Anisotropic wettability of laser micro-grooved SiC surfaces. *Applied surface science*, 284:930–935, 2013. ISBN: 0169-4332 Publisher: Elsevier.

[190] Yong, J., Yang, Q., Chen, F., Zhang, D., Farooq, U., Du, G., and Hou, X. A simple way to achieve superhydrophobicity, controllable water adhesion, anisotropic sliding, and anisotropic wetting based on femtosecond-laser-induced line-patterned surfaces. *Journal of Materials Chemistry A*, 2(15):5499–5507, 2014. Publisher: Royal Society of Chemistry.

[191] Wu, H., Zhang, R., Sun, Y., Lin, D., Sun, Z., Pan, W., and Downs, P. Biomimetic nanofiber patterns with controlled wettability. *Soft matter*, 4(12): 2429–2433, 2008.

[192] Parihar, V., Bandyopadhyay, S., Das, S., and Dasgupta, S. Anisotropic electrowetting on wrinkled surfaces: enhanced wetting and dependency on initial wetting state. *Langmuir*, 34(5):1844–1854, 2018. ISBN: 0743-7463 Publisher: ACS Publications.

[193] Li, P., Zhang, B., Zhao, H., Zhang, L., Wang, Z., Xu, X., Fu, T., Wang, X., Hou, Y., Fan, Y., et al. Unidirectional droplet transport on the biofabricated butterfly wing. *Langmuir*, 34(41):12482–12487, 2018.

[194] Kumar, C., Palacios, A., Surapaneni, V. A., Bold, G., Thielen, M., Licht, E., Higham, T. E., Speck, T., and Le Houérou, V. Replicating the complexity of natural surfaces: technique validation and applications for biomimetics, ecology and evolution. *Philosophical Transactions of the Royal Society A*, 377(2138): 20180265, 2019.

[195] Singab, A. N. B., Ayoub, I. M., El-Shazly, M., Korinek, M., Wu, T.-Y., Cheng, Y.-B., Chang, F.-R., and Wu, Y.-C. Shedding the light on iridaceae: Ethnobotany, phytochemistry and biological activity. *Industrial Crops and Products*, 92:308–335, 2016.

[196] Sun, G. and Fang, Y. Anisotropic characteristic of insect (lepidoptera) wing surfaces. In *International Conference on Logistics Engineering, Management and Computer Science (LEMCS 2015)*, pages 633–635. Atlantis Press, 2015.

[197] Parvate, S., Dixit, P., and Chattopadhyay, S. Superhydrophobic surfaces: insights from theory and experiment. *The Journal of Physical Chemistry B*, 124 (8):1323–1360, 2020. ISBN: 1520-6106 Publisher: ACS Publications.

[198] Chu, K.-H., Xiao, R., and Wang, E. N. Uni-directional liquid spreading on asymmetric nanostructured surfaces. *Nature materials*, 9(5):413–417, 2010.

[199] Choi, W., Tuteja, A., Mabry, J. M., Cohen, R. E., and McKinley, G. H. A modified Cassie–Baxter relationship to explain contact angle hysteresis and anisotropy on non-wetting textured surfaces. *Journal of colloid and interface science*, 339(1):208–216, 2009. ISBN: 0021-9797 Publisher: Elsevier.

[200] Kumar, M., Bhardwaj, R., and Sahu, K. C. Motion of a droplet on an anisotropic microgrooved surface. *Langmuir*, 35(8):2957–2965, 2019.

[201] Cottin-Bizonne, C., Barentin, C., Charlaix, ., Bocquet, L., and Barrat, J.-L. Dynamics of simple liquids at heterogeneous surfaces: Molecular-dynamics simulations and hydrodynamic description. *The European Physical Journal E*, 15:427–438, 2004. ISBN: 1292-8941 Publisher: Springer.

[202] Courbin, L. Rethinking Superhydrophobicity. *Physics*, 9:23, 2016. Publisher: APS.

[203] Smith, A. F., Mahelona, K., and Hendy, S. C. Rolling and slipping of droplets on superhydrophobic surfaces. *Physical Review E*, 98(3):033113, 2018. Publisher: APS.

[204] Richard, D. and Quéré, D. Viscous drops rolling on a tilted non-wettable solid. *Europhysics letters*, 48(3):286, 1999. ISBN: 0295-5075 Publisher: IOP Publishing.

[205] Backholm, M., Molpeceres, D., Vuckovac, M., Nurmi, H., Hokkanen, M. J., Jokinen, V., Timonen, J. V., and Ras, R. H. Water droplet friction and rolling dynamics on superhydrophobic surfaces. *Communications Materials*, 1(1):64, 2020.

[206] Yamamoto, M., Nishikawa, N., Mayama, H., Nonomura, Y., Yokojima, S., Nakamura, S., and Uchida, K. Theoretical explanation of the lotus effect: superhydrophobic property changes by removal of nanostructures from the surface of a lotus leaf. *Langmuir*, 31(26):7355–7363, 2015. ISSN 0743-7463. Publisher: ACS Publications.

[207] Song, D., Daniello, R. J., and Rothstein, J. P. Drag reduction using superhydrophobic sanded teflon surfaces. *Experiments in fluids*, 55:1–8, 2014.

[208] Perumanath, S., Pillai, R., and Borg, M. K. Contaminant removal from nature's self-cleaning surfaces. *Nano Letters*, 23(10):4234–4241, 2023.

[209] Lu, X., Peng, Y., Qiu, H., Liu, X., and Ge, L. Anti-fouling membranes by manipulating surface wettability and their anti-fouling mechanism. *Desalination*, 413:127–135, 2017.

[210] Cao, L., Jones, A. K., Sikka, V. K., Wu, J., and Gao, D. Anti-icing superhydrophobic coatings. *Langmuir*, 25(21):12444–12448, 2009.

[211] Chen, L. and Li, Z. Bouncing droplets on nonsuperhydrophobic surfaces. *Physical Review E—Statistical, Nonlinear, and Soft Matter Physics*, 82(1):016308, 2010.

[212] Tsai, P., Pacheco, S., Pirat, C., Lefferts, L., and Lohse, D. Drop impact upon micro-and nanostructured superhydrophobic surfaces. *Langmuir*, 25(20):12293–12298, 2009.

[213] Liu, Y., Whyman, G., Bormashenko, E., Hao, C., and Wang, Z. Controlling drop bouncing using surfaces with gradient features. *Applied Physics Letters*, 107(5), 2015.

[214] Guo, C., Zhao, D., Sun, Y., Wang, M., and Liu, Y. Droplet impact on anisotropic superhydrophobic surfaces. *Langmuir*, 34(11):3533–3540, 2018.

[215] Li, J., Oron, A., and Jiang, Y. Droplet jump-off force on a superhydrophobic surface. *Physical Review Fluids*, 8(11):113601, 2023.

[216] Shen, Y., Tao, J., Tao, H., Chen, S., Pan, L., and Wang, T. Relationship between wetting hysteresis and contact time of a bouncing droplet on hydrophobic surfaces. *ACS applied materials & interfaces*, 7(37):20972–20978, 2015.

[217] Xiu, Y., Zhu, L., Hess, D. W., and Wong, C. Relationship between work of adhesion and contact angle hysteresis on superhydrophobic surfaces. *The Journal of Physical Chemistry C*, 112(30):11403–11407, 2008.

[218] Pathan, A., Bond, J., and Gaskin, R. Sample preparation for sem of plant surfaces. *Materials Today*, 12:32–43, 2010.

[219] Lewicki, P. P. and Pawlak, G. Effect of drying on microstructure of plant tissue. *Drying technology*, 21(4):657–683, 2003.

[220] Guo, K., Liu, M., Vella, D., Suresh, S., and Hsia, K. J. Dehydration-induced corrugated folding in rhapis excelsa plant leaves. *Proceedings of the National Academy of Sciences*, 121(17):e2320259121, 2024.

[221] Kitajima, K., Wright, S. J., and Westbrook, J. W. Leaf cellulose density as the key determinant of inter-and intra-specific variation in leaf fracture toughness in a species-rich tropical forest. *Interface focus*, 6(3):20150100, 2016.

[222] Baldygin, A., Ahmed, A., Baily, R., Ismail, M. F., Khan, M., Rodrigues, N., Salehi, A.-R., Ramesh, M., Bhattacharya, S., Willers, T., et al. Effect of gravity on the spreading of a droplet deposited by liquid needle deposition technique. *npj Microgravity*, 9(1):49, 2023.

[223] Liu, T. . and Kim, C.-J. . Contact angle measurement of small capillary length liquid in super-repelled state. *Scientific reports*, 7(1):740, 2017.

[224] Ding, S., Hu, Z., Dai, L., Zhang, X., and Wu, X. Droplet impact dynamics on single-pillar superhydrophobic surfaces. *Physics of Fluids*, 33(10), 2021.

[225] Jung, Y. C. and Bhushan, B. Dynamic effects of bouncing water droplets on superhydrophobic surfaces. *Langmuir*, 24(12):6262–6269, 2008.

[226] McDonald, J. E. The shape and aerodynamics of large raindrops. *Journal of Atmospheric Sciences*, 11(6):478–494, 1954.

[227] Campbell, J. L., Breedon, M., Latham, K., and Kalantar-Zadeh, K. Electrowetting of superhydrophobic zno nanorods. *Langmuir*, 24(9):5091–5098, 2008.

[228] Lin, Y.-Y., Evans, R. D., Welch, E., Hsu, B.-N., Madison, A. C., and Fair, R. B. Low voltage electrowetting-on-dielectric platform using multi-layer insulators. *Sensors and Actuators B: Chemical*, 150(1):465–470, 2010.

[229] Yang, C., Zeng, Q., Huang, J., and Guo, Z. Droplet manipulation on superhydrophobic surfaces based on external stimulation: A review. *Advances in Colloid and Interface Science*, 306:102724, 2022.

[230] Biroun, M. H., Haworth, L., Agrawal, P., Orme, B., McHale, G., Torun, H., Rahmati, M., and Fu, Y. Surface acoustic waves to control droplet impact onto

superhydrophobic and slippery liquid-infused porous surfaces. *ACS Applied Materials & Interfaces*, 13(38):46076–46087, 2021.

[231] Geng, H., Feng, J., Stabryla, L. M., and Cho, S. K. Droplet manipulations by dielectrowetting: Creating, transporting, splitting, and merging. In *2017 IEEE 30th International Conference on Micro Electro Mechanical Systems (MEMS)*, pages 113–116. IEEE, 2017.

[232] Zhao, Y. and Cho, S. K. Micro air bubble manipulation by electrowetting on dielectric (ewod): transporting, splitting, merging and eliminating of bubbles. *Lab on a Chip*, 7(2):273–280, 2007.

[233] Huo, X., Li, L., Yang, Y., Liu, X., Yu, Q., and Wang, Q. The dynamics of directional transport of a droplet in programmable electrowetting channel. *Physics of Fluids*, 35(3), 2023.

[234] Krupenkin, T., Yang, S., and Mach, P. Tunable liquid microlens. *Applied physics letters*, 82(3):316–318, 2003.

[235] Li, L.-Y., Yuan, R.-Y., Wang, J.-H., Li, L., and Wang, Q.-H. Optofluidic lens based on electrowetting liquid piston. *Scientific Reports*, 9(1):13062, 2019.

[236] Zhang, D.-Y., Lien, V., Berdichevsky, Y., Choi, J., and Lo, Y.-H. Fluidic adaptive lens with high focal length tunability. *Applied physics letters*, 82(19): 3171–3172, 2003.

[237] Hendriks, B., Kuiper, S., Van As, M., Renders, C., and Tukker, T. Electrowetting-based variable-focus lens for miniature systems. *Optical review*, 12:255–259, 2005.

[238] Park, I., Yang, J., Oh, S., and Chung, S. Multifuctional liquid lens for high-performance miniature cameras. In *2016 IEEE 29th International Conference on Micro Electro Mechanical Systems (MEMS)*, pages 776–779. IEEE, 2016.

[239] Li, L., Liu, C., Peng, H.-R., and Wang, Q.-H. Optical switch based on electrowetting liquid lens. *Journal of Applied Physics*, 111(10), 2012.

[240] Petsch, S., Schuhladen, S., Dreesen, L., and Zappe, H. The engineered eyeball, a tunable imaging system using soft-matter micro-optics. *Light: Science & Applications*, 5(7):e16068–e16068, 2016.

[241] Liu, C.-X., Park, J., and Choi, J.-W. A planar lens based on the electrowetting of two immiscible liquids. *Journal of Micromechanics and Microengineering*, 18(3):035023, 2008.

[242] Park, J., Liu, C.-X., and Choi, J.-W. A planar liquid lens design based on electrowetting. In *SENSORS, 2007 IEEE*, pages 439–442. IEEE, 2007.

[243] Ghatak, A. *Optics*. New Delhi: Tata McGraw-Hill Higher Education, 2010.

[244] Svitova, T., Theodoly, O., Christiano, S., Hill, R., and Radke, C. Wetting behavior of silicone oils on solid substrates immersed in aqueous electrolyte solutions. *Langmuir*, 18(18):6821–6829, 2002.

[245] Cooper, E. F. and Asfour, A. F. A. Densities and kinematic viscosities of some c6-c16 n-alkane binary liquid systems at 293.15 k. *Journal of Chemical and Engineering Data*, 36(3):285–288, 1991.

[246] Ozkan, O. and Erbil, H. Y. Interpreting contact angle results under air, water and oil for the same surfaces. *Surface Topography: Metrology and Properties*, 5 (2):024002, 2017.

[247] Demond, A. H. and Lindner, A. S. Estimation of interfacial tension between organic liquids and water. *Environmental science & technology*, 27(12):2318–2331, 1993.

[248] Bi, X., Crum, B. P., and Li, W. Super hydrophobic parylene-c produced by consecutive o_2 and sf_6 plasma treatment. *Journal of Microelectromechanical Systems*, 23(3):628–635, 2013.

[249] Neelakantan, N. K., Weisensee, P. B., Overcash, J. W., Torrealba, E. J., King, W. P., and Suslick, K. S. Spray-on omniphobic zno coatings. *RSC advances*, 5 (85):69243–69250, 2015.

[250] Gao, L. and McCarthy, T. J. Teflon is hydrophilic. comments on definitions of hydrophobic, shear versus tensile hydrophobicity, and wettability characterization. *Langmuir*, 24(17):9183–9188, 2008.

[251] Zhang and Han. Viscosity and density of water+ sodium chloride+ potassium chloride solutions at 298.15 k. *Journal of Chemical & Engineering Data*, 41(3): 516–520, 1996.

[252] Ren, W. et al. Boundary conditions for the moving contact line problem. *Physics of fluids*, 19(2), 2007.

[253] Ren, W., Hu, D., et al. Continuum models for the contact line problem. *Physics of fluids*, 22(10), 2010.

[254] Scardovelli, R. and Zaleski, S. Direct numerical simulation of free-surface and interfacial flow. *Annual review of fluid mechanics*, 31(1):567–603, 1999.

[255] Blesgen, T. A generalization of the navier-stokes equations to two-phase flows. *Journal of Physics D: Applied Physics*, 32(10):1119, 1999.

[256] Katopodes, N. D. *Free-Surface Flow:: Shallow Water Dynamics*. Butterworth-Heinemann, 2018.

[257] Brackbill, J. U., Kothe, D. B., and Zemach, C. A continuum method for modeling surface tension. *Journal of computational physics*, 100(2):335–354, 1992.

[258] Multiphysics, C. et al. Comsol multiphysics reference manual. *COMSOL: Grenoble, France*, 1084:834, 2013.

[259] Peng, R., Wang, D., Hu, Z., Chen, J., and Zhuang, S. Focal length hysteresis of a double-liquid lens based on electrowetting. *Journal of optics*, 15(2):025707, 2013.

[260] Tayel, S. A., Abu El-Maaty, A. E., Mostafa, E. M., and Elsaadawi, Y. F. Enhance the performance of photovoltaic solar panels by a self-cleaning and hydrophobic nanocoating. *Scientific reports*, 12(1):21236, 2022.

[261] Chakrapani Gunarasan, J. P. and Lee, J.-W. Active surface area-dependent water harvesting of desert beetle-inspired hybrid wetting surfaces. *Langmuir*, 40(10):5499–5507, 2024.

[262] Wang, J., Chen, Y., Xu, Q., Cai, M., Shi, Q., and Gao, J. Highly efficient reusable superhydrophobic sponge prepared by a facile, simple and cost effective biomimetic bonding method for oil absorption. *Scientific Reports*, 11(1):11960, 2021.

[263] Latip, E. A., Coudron, L., McDonnell, M., Johnston, I., McCluskey, D., Day, R., and Tracey, M. Protein droplet actuation on superhydrophobic surfaces: a new approach toward anti-biofouling electrowetting systems. *Rsc Advances*, 7 (78):49633–49648, 2017.

[264] Roth-Nebelsick, A. and Krause, M. The plant leaf: A biomimetic resource for multifunctional and economic design. *Biomimetics*, 8(2):145, 2023.

[265] Bhushan, B. *Biomimetics: bioinspired hierarchical-structured surfaces for green science and technology*. Springer, 2016.

[266] Zhang, J., Li, J., and Han, Y. Superhydrophobic ptfe surfaces by extension. *Macromolecular Rapid Communications*, 25(11):1105–1108, 2004.

[267] Khorasani, M., Mirzadeh, H., and Kermani, Z. Wettability of porous polydimethylsiloxane surface: morphology study. *Applied Surface Science*, 242(3-4): 339–345, 2005.

[268] Ma, M., Hill, R. M., Lowery, J. L., Fridrikh, S. V., and Rutledge, G. C. Electrospun poly (styrene-block-dimethylsiloxane) block copolymer fibers exhibiting superhydrophobicity. *Langmuir*, 21(12):5549–5554, 2005.

[269] Bormashenko, E., Stein, T., Whyman, G., Bormashenko, Y., and Pogreb, R. Wetting properties of the multiscaled nanostructured polymer and metallic superhydrophobic surfaces. *Langmuir*, 22(24):9982–9985, 2006.

[270] Lee, W., Jin, M.-K., Yoo, W.-C., and Lee, J.-K. Nanostructuring of a polymeric substrate with well-defined nanometer-scale topography and tailored surface wettability. *Langmuir*, 20(18):7665–7669, 2004.

[271] Hikita, M., Tanaka, K., Nakamura, T., Kajiyama, T., and Takahara, A. Superliquid-repellent surfaces prepared by colloidal silica nanoparticles covered with fluoroalkyl groups. *Langmuir*, 21(16):7299–7302, 2005.

[272] Bhushan, B., Koch, K., and Jung, Y. C. Nanostructures for superhydrophobicity and low adhesion. *Soft Matter*, 4(9):1799–1804, 2008.

[273] Klein, R. J., Maarten Biesheuvel, P., Yu, B. C., Meinhart, C. D., and Lange, F. F. Producing super-hydrophobic surfaces with nano-silica spheres. *International Journal of Materials Research*, 94(4):377–380, 2022.

[274] Zhang, X., Shi, F., Yu, X., Liu, H., Fu, Y., Wang, Z., Jiang, L., and Li, X. Polyelectrolyte multilayer as matrix for electrochemical deposition of gold clusters: toward super-hydrophobic surface. *Journal of the American chemical society*, 126(10):3064–3065, 2004.

[275] Jung, Y. C. and Bhushan, B. Mechanically durable carbon nanotube- composite hierarchical structures with superhydrophobicity, self-cleaning, and low-drag. *ACS nano*, 3(12):4155–4163, 2009.

[276] Feng, X., Feng, L., Jin, M., Zhai, J., Jiang, L., and Zhu, D. Reversible superhydrophobicity to super-hydrophilicity transition of aligned zno nanorod films. *Journal of the American Chemical Society*, 126(1):62–63, 2004.